Electronics and Electrical Engineering

https://www.aimspress.com/journal/ElectrEng

AIMS Electronics and Electrical Engineering, 10(3): 422–445
DOI: 10.3934/electreng.2026017
Received: 19 December 2025
Revised: 28 March 2026
Accepted: 27 April 2026
Published: 04 June 2026

Research article

Adaptive speed control of a converter-driven DC motor

Said Oucheriah and Abul Azad*

Department of Engineering Technology, Northern Illinois University, DeKalb, IL 60115, USA

* **Correspondence:** Email: aazad@niu.edu.

Abstract: Numerous studies have appeared in the control literature regarding the regulation of the angular speed of DC motors driven by DC-DC converters. In this work, we considered a buck converter-driven DC motor system. The implementation of the proposed adaptive controller requires only one sensor to measure the motor angular speed. An estimator was developed to estimate the inductor current and the output voltage of the converter, the armature current of the DC motor, and to generate a simple adaptation law for the estimate of the external load torque. A linear sliding surface was used to derive an adaptive controller that is simple in its design and guarantees closed-loop system stability and precise speed regulation in the presence of the inductor parasitic and parameter uncertainties of the converter/motor system. Furthermore, the controller was shown to be robust against external disturbances. A simple systematic procedure was outlined to select the three gains of the proposed adaptive controller. The robustness and effectiveness of the controller were validated by computer simulations and compared to the proportional integral derivative (PID) control.

Keywords: DC-DC buck converter; adaptive speed control; observer; DC motors

1. Introduction

Numerous design techniques have appeared in the control literature dealing with the regulation of the angular speed of DC motors driven by DC-DC converters in the areas of robotics, renewable energy, and electric vehicles.

Flatness and passivity-based controllers are non-linear control techniques that have been used to achieve precise speed regulation in DC motors. A velocity-sensorless tracking control approach based on the exact tracking error dynamics passive output feedback scheme was proposed for a buck-boost converter in [1] and a full-bridge buck inverter–DC motor system in [9] that considered only inductor current sensing and used some reference trajectories for the systems. The robustness of both controllers was tested only for the case of an abrupt change of the load resistance of the converter and resulted in a significant steady-state error between the actual speed and the reference speed.

In [10], a robust differential flatness-based tracking control for the full-bridge buck inverter–DC motor was developed where the controller robustness was shown only for variations of the load resistance of the converter and ignoring uncertainties of all the other parameters of the system. Furthermore, missing in these three studies was the inclusion of an external load torque that is present in real systems. In [15], a two-level hierarchical control that treats the converter and the DC motor as two independent subsystems was proposed with a high-level control for the motor and a low-level control for the converter using the differential flatness property. Here also, the external torque was omitted in the model and the robustness of the controller was tested only for the case of abrupt changes of the load and capacitor of the converter.

In [20], an adaptive passivity-based controller was proposed to regulate the angular speed of the DC motor system fed by a DC-DC converter using an incremental port-Hamiltonian representation. The unknown external load torque was estimated using a nonlinear disturbance observer. The implementation of the controller for the boost converter required four sensors.

All the controllers proposed above rely on the exact knowledge of the converter/motor system parameters. There were not tested for robustness to parasitics and parameter uncertainties that exist in practice, especially the ones associated with the motor.

Other control strategies for DC motor speed control are the proportional integral derivative (PID)-based schemes to improve transients and steady-state behavior, which are also known for their very simple implementation. In [11], a PID controller was used to control the speed of a DC motor and a Kalman filter was used to reduce the noise from the speed sensor. In [24], smooth voltage trajectory planning based on Bézier curves was used to reduce high voltages and current peaks during step speed transitions. The fixed gains of these conventional PID controllers may drastically degrade their performance during the presence of external disturbances and changes of operating points. To remedy the fixed gain problem, PID gains were optimally tuned using heuristic optimization methods [3–6, 12] to improve tracking accuracy, robustness to parameter uncertainties, and performance in terms of the disturbance rejection capability. However, their designs can be complex and their algorithms computationally intensive that render a real-time implementation very challenging and not practical for systems with low processing capabilities. Furthermore, these high computational intensity heuristic algorithms may hinder the reaching of optimal stable points due to delay times in control actions during rapid transition changes in the system.

Model predictive control (MPC) strategies have emerged as powerful robust control schemes for precise speed regulation of DC motors [2,21–23]. MPC uses a prediction model and solves in real-time an optimization problem to determine optimal control actions. The control algorithms require extensive computations, an online complex optimization problem that may require nonlinear programming techniques, and a large number of parameters to be tuned with some chosen in an ad-hoc manner. It also requires accurate system modeling with degradation of performance with parameter uncertainties and external disturbances. This makes them of little practical interest and unsuitable for systems with low processing capabilities.

Sliding mode control (SMC) has been used for DC motor speed control and offers exceptional robustness to external load disturbances and parameter uncertainties, high accuracy, and fast dynamic response. In [8], a continuous dynamic sliding mode control technique that addresses parametric uncertainties of the converter/motor system was proposed. Four different third-order finite-time disturbance observers (FTDOs) were proposed to estimate four lumped uncertainties and their higher

derivatives. Each observer had four different gains and the controller had four different design coefficients and a gain. No procedure was given in the selection of the 21 design parameters. In [13], the control strategy consisted of multiple proportional-integral (PI) loops for velocity control, armature current control, and converter capacitor voltage control, and a sliding mode loop designed to regulate the current of the converter. However, the robustness of the controller was tested only for the case of step changes of the input voltage, the load, and the capacitor of the converter with only local asymptotic stability of the equilibrium addressed. In [14], controllers based on a third-order classical sliding surface and a proportional integral derivative sliding surface were proposed for the speed regulation of the DC motor fed by the buck converter with some design parameters chosen by trial-and-error and trials and with some having very large values. Moreover, the controller was composed of a continuous component and a discontinuous one that can lead to chattering problems. In [8, 13, 14], the implementation of each controller required four sensors. In [16], a sliding mode controller (SMC) optimized using a genetic algorithm (GA) and particle swarm optimization (PSO) was proposed. Although the proposed controller improved robustness to disturbances and parameter uncertainties, its implementation required intensive and time consuming computations that make it impractical and unsuitable for systems with low processing capabilities.

In [17], an adaptive inverse optimal control (IOC) scheme was used to regulate the speed of a DC motor system fed by a DC/DC converter. A disturbance observer (DO) was used to estimate the external load torque. However, no robustness analysis and/or simulations on parameter uncertainties were done considering that the controller and the disturbance observer were strongly dependent on the converter-motor system parameters. Moreover, the implementation of the IOC controller required four sensors.

Fuzzy logic control of DC motor speed control [7, 18, 19] does not require precise knowledge of the dynamic model of the controlled system. It offers very precise reference motor speed tracking with robustness to unknown nonlinear dynamics, parameter uncertainties, and external disturbances. However, the control strategy involves intensive training with complex subjective tuning of fuzzy rules that result in time delays of the control actions and thus a degradation of the system performance for fast transients. This control scheme is computationally very intensive and lacks a systematic design approach thus rendering a real-time implementation impossible for systems with low processing capabilities.

While many of these approaches effectively address the issue of speed regulation of converter-driven DC motors, they often have limitations. Achieving robust and stable speed control of motors under time-varying disturbances and parameter uncertainties with a simple controller remains a persistent challenge. The adaptive sliding mode controller proposed here addresses most of the above limitations.

1) The adaptive controller requires only one sensor to measure the angular speed of the motor for its implementation, thus saving a voltage sensor, two current sensors, and a torque sensor.

2) A linear sliding surface is used to derive a controller that is very simple in its design and requires only three design parameters for its implementation. A detailed analysis of the closed-loop stability for nominal parameters is presented. A simple procedure is developed to systematically determine the values of two gains. The third gain, which is an adaptation law gain, is determined by tuning.

3) The use of estimated values in the implementation of the proposed controller filters much of the noise present in the original states, significantly enhancing the system's noise robustness and resulting in a major reduction in chattering.

4) The robustness of the proposed controller to parameter uncertainties and parasitics of the converter/motor system is validated through numerous simulations that show that despite the presence of large parameter variations, the controller yields accurate angular speed tracking.

Standard PID-based controllers are still widely used in industry and are shown to achieve precise speed control under varying load torques and parameter uncertainties. They require one sensor and are very simple to implement. This makes the PID controller suitable for comparison with the proposed adaptive controller.

2. Dynamic model of the buck converter/DC motor system

A basic buck converter/DC motor system is shown in Figure 1.

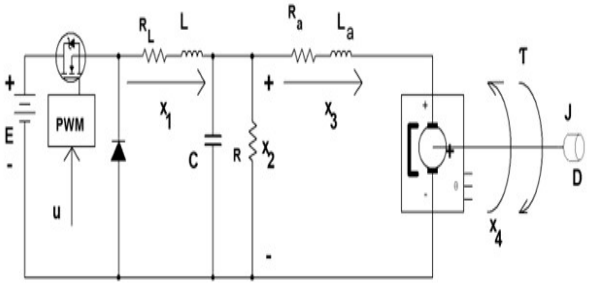

Figure 1. Circuit diagram of the buck converter/DC motor system.

Using Kirchhoff and Newton's second law of mechanics, the dynamic model of the system is

$$\begin{aligned} \dot{x}_1 &= -\frac{R_L}{L}x_1 - \frac{x_2}{L} + u\frac{E}{L} \\ \dot{x}_2 &= \frac{x_1}{C} - \frac{x_2}{RC} - \frac{x_3}{C} \\ \dot{x}_3 &= \frac{x_2}{L_a} - \frac{R_a}{L_a}x_3 - \frac{k_e}{L_a}x_4 \\ \dot{x}_4 &= \frac{k_m}{J}x_3 - \frac{D}{J}x_4 - \frac{\tau}{J} \end{aligned} \tag{1}$$

where x_1 represents the average inductor current of the buck converter, x_2 is the average voltage across the load resistor R, x_3 is the armature current of the motor, and x_4 denotes the angular speed of the motor shaft. For the buck converter, the parameters E, L, C, and R represent the input voltage, the inductance, the capacitance, and the load resistance, respectively. The parasitic R_L represents the inductor equivalent series resistance, and the control input u to the converter is the duty ratio function.

For the DC motor, R_a represents the armature resistance, L_a is the inductance of the DC motor, and τ is the load torque. The parameters J, k_e, k_m, and D represent the inertia, the electromotive force, the torque constant and the viscous friction coefficient, respectively.

The objective here is to regulate the angular speed of the motor to a desired speed $x_4 = x_4^* = \omega_{ref}$.

Setting the derivatives of (1) to zeros yields the following equilibrium:

$$\begin{aligned} x_1^* &= \frac{x_2^*}{R} + x_3^* \\ x_2^* &= R_a x_3^* + k_e x_4^* \\ x_3^* &= \frac{D x_4^* + \tau}{k_m} \\ u^* &= \frac{x_2^* + R_L x_1^*}{E} \end{aligned} \tag{2}$$

2.1. Estimator and adaptation law

The load torque τ is unknown and assumed piecewise constant. An estimator is used to facilitate the design of the parameter adaptation law for the estimate of τ and also estimates x_1 and x_2, the average inductor current of the buck converter and the output voltage across R, respectively, and x_3, the armature current. To this end, the following estimator is considered.

$$\begin{aligned} \dot{\hat{x}}_1 &= -\frac{R_L}{L}\hat{x}_1 - \frac{\hat{x}_2}{L} + u\frac{E}{L} \\ \dot{\hat{x}}_2 &= \frac{\hat{x}_1}{C} - \frac{\hat{x}_2}{RC} - \frac{\hat{x}_3}{C} \\ \dot{\hat{x}}_3 &= \frac{\hat{x}_2}{L_a} - \frac{R_a}{L_a}\hat{x}_3 - \frac{k_e}{L_a}\hat{x}_4 \\ \dot{\hat{x}}_4 &= \frac{k_m}{J}\hat{x}_3 - \frac{D}{J}\hat{x}_4 - \frac{\hat{\tau}}{J} + K_4(x_4 - \hat{x}_4) \end{aligned} \tag{3}$$

where $\hat{x}_1, \hat{x}_2, \hat{x}_3, \hat{x}_4$, and $\hat{\tau}$ are the estimates of x_1, x_2, x_3, x_4, and τ, respectively, and $K_4 > 0$ is the estimator gain. Using (1) and (3) yields the following error equations:

$$\begin{aligned} \dot{\tilde{x}}_1 &= -\frac{R_L}{L}\tilde{x}_1 - \frac{\tilde{x}_2}{L} \\ \dot{\tilde{x}}_2 &= \frac{\tilde{x}_1}{C} - \frac{\tilde{x}_2}{RC} - \frac{\tilde{x}_3}{C} \\ \dot{\tilde{x}}_3 &= \frac{\tilde{x}_2}{L_a} - \frac{R_a}{L_a}\tilde{x}_3 - \frac{k_e}{L_a}\tilde{x}_4 \\ \dot{\tilde{x}}_4 &= \frac{k_m}{J}\tilde{x}_3 - \left[\frac{D}{J} + K_4\right]\tilde{x}_4 - \frac{\tilde{\tau}}{J} \end{aligned} \tag{4}$$

where $\tilde{x}_1 = x_1 - \hat{x}_1,\ \tilde{x}_2 = x_2 - \hat{x}_2,\ \tilde{x}_3 = x_3 - \hat{x}_3,\ \tilde{x}_4 = x_4 - \hat{x}_4$, and $\tilde{\tau} = \tau - \hat{\tau}$ are the estimation errors.

Remark 1: In addition to a major reduction in sensors, another advantage of the use of estimated states in the implementation of the controller is the filtering of much of the high-frequency noise present in the original states, significantly enhancing the system noise robustness and showing a major reduction in chattering.

To generate the adaptation law for the estimate of the load torque τ, we consider the following quadratic Lyapunov function:

$$V = \frac{1}{2}L\tilde{x}_1^2 + \frac{1}{2}C\tilde{x}_2^2 + \frac{1}{2}L_a\tilde{x}_3^2 + \frac{Jk_e}{2k_m}\tilde{x}_4^2 + \frac{1}{2\gamma}\tilde{\tau}^2 \tag{5}$$

where $\gamma > 0$ is a design parameter. Its time derivative along the solutions of (4) is

$$\begin{aligned}\dot{V} = -R_L\tilde{x}_1^2 - \frac{1}{R}\tilde{x}_2^2 - R_a\tilde{x}_3^2 - \frac{Jk_e}{k_m}\left[\frac{D}{J} + K_4\right]\tilde{x}_4^2 \\ - \tilde{\tau}\left[\frac{k_e}{k_m}\tilde{x}_4 + \frac{\dot{\hat{\tau}}}{\gamma}\right]\end{aligned} \tag{6}$$

The adaptation law is determined by canceling the term in the brackets and is given by

$$\dot{\hat{\tau}} = -\gamma\frac{k_e}{k_m}\tilde{x}_4 \tag{7}$$

With the adaptation law (7), we now have

$$\dot{V} = -R_L\tilde{x}_1^2 - \frac{1}{R}\tilde{x}_2^2 - R_a\tilde{x}_3^2 - \frac{Jk_e}{k_m}\left[\frac{D}{J} + K_4\right]\tilde{x}_4^2 \tag{8}$$

In view of (8) and using the Lasalle invariant principle, we can conclude that $\tilde{x}_1 \to 0,\ \tilde{x}_2 \to 0,\ \tilde{x}_3 \to 0$, and $\tilde{x}_4 \to 0$ asymptotically. Since $\tilde{\tau} \to 0$, we also have $\hat{\tau} \to \tau$.

2.2. Control law design

Since the equilibrium point given in (2) depends on the torque τ, which is unknown, its estimate is determined by replacing τ in (2) by its estimate $\hat{\tau}$ to yield

$$\begin{aligned}\hat{x}_1^* &= \frac{\hat{x}_2^*}{R} + \hat{x}_3^* \\ \hat{x}_2^* &= R_a\hat{x}_3^* + k_e x_4^* \\ \hat{x}_3^* &= \frac{Dx_4^* + \hat{\tau}}{k_m} \\ \hat{u}^* &= \frac{\hat{x}_2^* + R_L\hat{x}_1^*}{E}\end{aligned} \tag{9}$$

Remark 2: The estimated equilibrium point converges to the true equilibrium point since $\hat{\tau} \to \tau$. We also have $\dot{\hat{x}}_1^* \to 0,\ \dot{\hat{x}}_2^* \to 0$, and $\dot{\hat{x}}_3^* \to 0$ since $\dot{x}_4^* = 0$ and $\dot{\hat{\tau}} \to 0$.

We consider the following sliding surface:

$$\sigma = \hat{x}_1 - \hat{x}_1^* \tag{10}$$

Using the expressions of the second and third equations of (9) in the first equation of (9) yields

$$\hat{x}_1^* = \alpha\left(Dx_4^* + \hat{\tau}\right) + \frac{k_e}{R}x_4^* \tag{11}$$

where

$$\alpha = \frac{\left(1 + \frac{R_a}{R}\right)}{k_m} \tag{12}$$

The controller u is derived by differentiating σ with respect to time and setting $\dot{\sigma} = 0$. Using (3), (7), (10), and (11), the controller u is given by

$$\begin{aligned} u &= \frac{\hat{x}_2 + R_L\hat{x}_1 + L\dot{\hat{x}}_1^*}{E} - \frac{K_s}{E}\sigma \\ &= \frac{\hat{x}_2 + R_L\hat{x}_1 + L\alpha\dot{\hat{\tau}}}{E} - \frac{K_s}{E}\sigma \\ &= \frac{\left(\hat{x}_2 + R_L\hat{x}_1 - \alpha L\gamma\dfrac{k_e}{k_m}\tilde{x}_4\right)}{E} - \frac{K_s}{E}\sigma \end{aligned} \tag{13}$$

The last term of the controller u is added to ensure the sliding mode condition. The substitution of the controller (13) into the derivative of (10) leads to

$$\dot{\sigma} = -\frac{K_s}{L}\,\sigma \tag{14}$$

and therefore we have $\dot{\sigma}\sigma = -\dfrac{K_s}{L}\sigma^2 < 0$, which ensures the sliding mode condition. Equation (14) admits as a solution

$$\sigma(t) = \sigma(0)e^{-\frac{K_s}{L}t} \tag{15}$$

For a choice of the initial condition of the load torque $\hat{\tau}(0)$, the initial condition of the estimate $\hat{x}_1(0)$ is selected to guarantee the occurrence of the sliding mode at $t = 0$ with the reaching phase completely eliminated with

$$\hat{x}_1(0) = \hat{x}_1^*(0) = \alpha\left(Dx_4^* + \hat{\tau}(0)\right) + \frac{k_e}{R}x_4^* \tag{16}$$

This yields $\sigma(0) = 0$ and in view of (15), $\sigma(t) = 0$ for all $t \geq 0$. In this case, we have

$$\hat{x}_1(t) = \hat{x}_1^* = \frac{\hat{x}_2^*}{R} + \hat{x}_3^*,\ t \geq 0 \tag{17}$$

Given $\hat{\tau}(0)$, and using (9), the other initial conditions of the estimator can be chosen as

$$\hat{x}_2(0) = \hat{x}_2^*(0),\ \hat{x}_3(0) = \hat{x}_3^*(0),\ \hat{x}_4(0) = x_4^* = \omega_{ref} \tag{18}$$

2.3. Stability analysis

Let

$$\begin{aligned} e_1 = \hat{x}_1 - \hat{x}_1^*,\ e_2 = \hat{x}_2 - \hat{x}_2^*, \\ e_3 = \hat{x}_3 - \hat{x}_3^*,\ e_4 = \hat{x}_4 - x_4^* \end{aligned} \tag{19}$$

In view of (17), we have $\hat{x}_1 = \hat{x}_1^*,\ t \geq 0$, and therefore,

$$e_1 = 0,\ \ t \geq 0 \tag{20}$$

Using the substitutions $\hat{x}_1 = \hat{x}_1^*,\ \hat{x}_2 = \hat{x}_2^* + e_2,\ \hat{x}_3^* = \hat{x}_3 + e_3$ in the second equation of (3) yields

$$\dot{e}_2 = \frac{\hat{x}_1^*}{C} - \frac{(\hat{x}_2^* + e_2)}{RC} - \frac{(\hat{x}_3^* + e_3)}{C} - \dot{\hat{x}}_2^* \tag{21}$$

Using the first equation of (9) yields

$$\dot{e}_2 = -\frac{e_2}{RC} - \frac{e_3}{C} - \dot{\hat{x}}_2^* \tag{22}$$

Using the substitutions $\hat{x}_2 = e_2 + \hat{x}_2^*$, $\hat{x}_3 = e_3 + \hat{x}_3^*$, and $\hat{x}_4 = e_4 + x_4^*$ in the third equation of (3) yields

$$\begin{aligned}\dot{e}_3 &= \frac{(e_2 + \hat{x}_2^*)}{L_a} - \frac{R_a}{L_a}(e_3 + \hat{x}_3^*) - \frac{k_e}{L_a}(e_4 + x_4^*) - \dot{\hat{x}}_3^* \\ &= \frac{e_2}{L_a} - \frac{R_a}{L_a}e_3 - \frac{1}{L_a}(R_a\hat{x}_3 + k_e x_4^* - \hat{x}_2^*) \\ &\qquad - \frac{k_e}{L_a}e_4 - \dot{\hat{x}}_3^*\end{aligned} \tag{23}$$

Using the second equation of (9) yields

$$\dot{e}_3 = \frac{e_2}{L_a} - \frac{R_a}{L_a}e_3 - \frac{k_e}{L_a}e_4 - \dot{\hat{x}}_3^* \tag{24}$$

Using the substitutions $\hat{x}_3 = e_3 + \hat{x}_3^*$ and $\hat{x}_4 = e_4 + x_4^*$ in the fourth equation of (3) yields

$$\begin{aligned}\dot{e}_4 &= \frac{k_m}{J}(e_3 + \hat{x}_3^*) - \frac{D}{J}(e_4 + x_4^*) - \frac{\hat{\tau}}{J} + K_4\tilde{x}_4 - \dot{x}_4^* \\ &= \frac{k_m}{J}e_3 - \frac{D}{J}e_4 + \frac{(k_m\hat{x}_3^* - Dx_4^* - \hat{\tau})}{J} + K_4\tilde{x}_4 - \dot{x}_4^*\end{aligned} \tag{25}$$

Using the third equation of (9) with $\dot{x}_4^* = 0$ yields

$$\dot{e}_4 = \frac{k_m}{J}e_3 - \frac{D}{J}e_4 + K_4\tilde{x}_4 \tag{26}$$

We consider the following quadratic Lyapunov function

$$V = \frac{1}{2}\,Ce_2^2 + \frac{1}{2}\,L_a e_3^2 + \frac{Jk_e}{2k_m}e_4^2 \tag{27}$$

Its time derivative along the solutions of (22), (24), and (26) is

$$\dot{V} = -\frac{1}{R}e_2^2 - R_a e_3^2 - \frac{Dk_e}{k_m}e_4^2 + \Psi_1 \tag{28}$$

where

$$\Psi_1 = -Ce_2\dot{\hat{x}}_2^* - L_a e_3\dot{\hat{x}}_3^* + K_4\frac{Jk_e}{k_m}e_4\tilde{x}_4 \tag{29}$$

Since $\tilde{x}_4 \to 0$, and in view of Remark 2, we also have $\dot{\hat{x}}_2^* \to 0$ and $\dot{\hat{x}}_3^* \to 0$, and therefore $\Psi_1 \to 0$. This implies that $e_1 = 0$, $e_2 \to 0$, $e_3 \to 0$, and $e_4 \to 0$, and finally the states x_1, x_2, x_3, and x_4 converge asymptotically to their respective equilibrium given by (2).

Remark 3: A few general guidelines for the choice of the controller and estimator gains are:

1) Choose $K_s = 1$.

2) To ensure that the estimator has much faster dynamics than the controlled feedback system, the gain of the estimator K_4 can be chosen as

$$K_4 = \frac{5}{\tau_m} \tag{30}$$

where

$$\tau_m = \frac{JR_a}{k_e k_m} \tag{31}$$

is the mechanical time constant of the motor.

3) The gain of the adaptive law given γ in (7) for the load torque estimate should be tuned, starting with a lower gain and increasing it until the output transient response is satisfactory during the start-up phase while maintaining $\hat{\tau} > 0$ and no overshoot occurs during step load torque changes. The higher the gain, the faster the convergence of the estimate to the external load torque. However, if the gain is too high, there will be oscillations in the output response, especially during load torque disturbances and extreme parameter variations.

3. Simulation results

To validate the performance of the proposed adaptive controller, comparison simulations are performed using the nominal buck/motor parameters shown in Table 1 in the design of the proposed controller and the PID controller. The motor parameters are taken from [2].

In order to achieve fair performance comparisons of the two controllers, the gains of the PID controller are tuned such that the speed tracking performances of the two controllers are closely similar in the absence of disturbances and parameter uncertainties. This will ensure a fair comparison of the robustness of the two controllers to external disturbances and parameter uncertainties.

Starting with an initial reference angular speed of 200 rad/s, the motor is subjected to step reference speed changes from 200 rad/s to 300 rad/s at t = 1 s, from 300 rad/s to 400 rad/s at t = 2 s, and then back to 200 rad/sec at t = 3 s. In this case, we assume that the parameters of the converter/motor system are known accurately and the motor is subjected to a constant load torque τ=0.1 N.m with E = 50 V.

In view of Remark 3, the estimator/controller gains are

$$K_4 = 518.41,\ K_s = 1,\ \gamma = 250 \tag{32}$$

For $\hat{\tau}(0) = 0$, the initial conditions for the estimator are obtained by using (9), (16), and (18).

The PID controller is

$$u = K_p\, e(t) + K_i \int_0^t e(\tau)\, d\tau + K_d\, \frac{de(t)}{dt} \tag{33}$$

where K_p, K_i, and K_d are the proportional, integral, and derivative gains, respectively, and $e = x_4^* - x_4$. The tuning of the PID controller gains yields

$$K_p = 1.8 \times 10^{-3},\ K_i = 0.06,\ K_d = 5 \times 10^{-6} \tag{34}$$

Table 1. Buck/motor nominal parameters.

Nominal Parameters	Values and Units
Voltage supply	$E = 50$ V
Capacitor	$C = 250\ \mu$F
Buck inductance	$L = 1$ mH
Inductor series resistance	$R_L = 0.5\ \Omega$
Load resistance	$R = 10\ \Omega$
Counter electromotive force constant	$k_e = 0.0699$ V/(rad/s)
Torque constant	$k_m = 0.0699$ N.m/A
Armature resistance	$R_a = 1.45\ \Omega$
Armature inductance	$L_a = 2$ mH
Viscuous friction coefficient	$D = 65.12 \times 10^{-6}$ N.m/(rad/s)
Motor inertia	$J = 32.5 \times 10^{-6}$ kg$-m^2$

As seen in Figure 2, both controllers yield almost identical responses with the angular velocity x_4 of the motor tightly tracking the reference speed with zero steady-state error and small settling times during step speed changes. The PID has a slightly smaller rise time than the proposed controller during speed step changes but a slightly larger rise and settling times during the start-up phase. Figure 3 depicts both controllers.

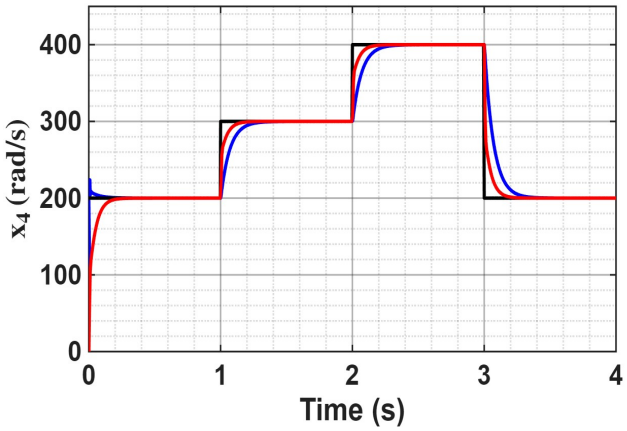

Figure 2. Angular speed responses. In black is the reference angular speed ω_{ref}, in blue is the angular speed x_4 using the proposed controller, and in red is the angular speed response x_4 using the PID controller.

In the next simulation, the motor is subjected to a time-varying angular speed reference of the form

$$\omega_{ref} = 200 + 100\ sin(0.4\pi t) \tag{35}$$

with $\tau = 0.1$ N.m, and E = 50 V, and assuming the nominal parameter values of Table 1. As shown in Figure 4, both controllers yield good speed tracking performances for the time-varying reference speed. Figure 5 depicts both controllers.

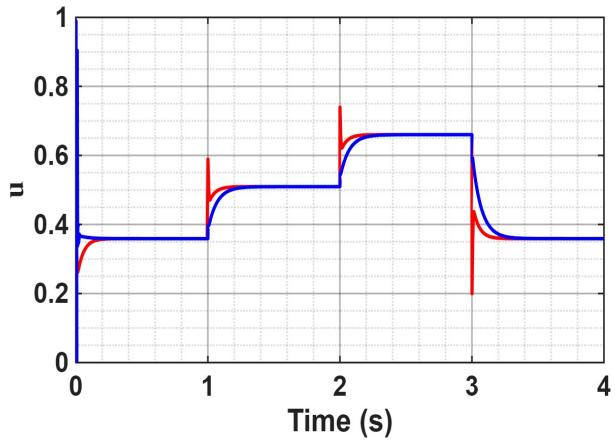

Figure 3. Duty ratio u. In blue is the proposed duty ratio and in red is the PID duty ratio.

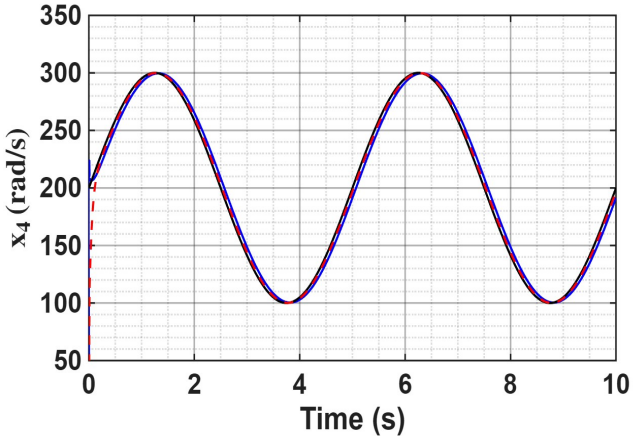

Figure 4. Angular speed responses. In black is the reference angular speed ω_{ref}, in blue is the response due to the proposed controller, and in red is the response due to the PID controller.

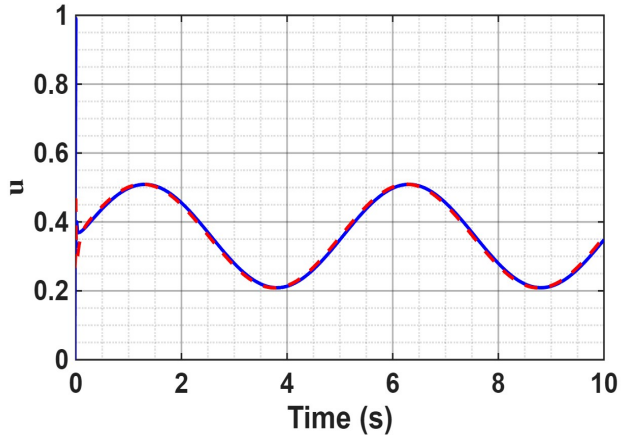

Figure 5. Duty ratio u. In blue is the proposed duty ratio and in red is the PID duty ration.

3.1. Case I—Robustness to sudden input voltage changes with parameter uncertainties

To test the robustness of the two controllers to step input voltage changes with parameter uncertainties, we assume that that the converter is subjected to an input voltage change from 50 V to 40 V at t = 1 s and then back to 50 V at t = 2 s with the converter/motor system subjected to the large parameter variations listed in Table 2. The reference angular speed is ω_{ref} = 200 rad/s and the load torque τ = 0.1 N.m.

Table 2. Buck/motor parameter uncertainties.

Actual values, increase/decrease in red
C = 350 μF **(+40 %)**
L = 800 μH **(-20 %)**
R_L = 1 Ω **(+100%)**
R = 13 Ω **(+30%)**
k_e = 0.03495 V/(rad/s) **(-50%)**
k_m = 0.04194 Nm/A **(-40 %)**
R_a = 2.465 Ω **(+70 %)**
L_a = 1.4 mH **(-30 %)**
$D = 104.192 \times 10^{-6}$ Nm/(rad/s) **(+60 %)**
$J = 16.25 \times 10^{-6}$ kg$-m^2$ **(-50 %)**

To evaluate the performance of the two controllers, the metrics used include the overshoot (OS), the undershoot (US), and the maximum settling time T_s. Here, we are using the 1% settling time to measure the recovery time.

The plots of the transient output responses are depicted in Figures 6 and 7. Using the proposed adaptive control, the motor speed undergoes a maximum deviation of 3.12 rad/s (1.56%) with the disturbance completely rejected in less than 21 ms. Using the PID controller, the motor speed undergoes a maximum deviation of 24 rad/s (12%) with the disturbance completely rejected in less than 125 ms. Table 3 summarizes the performances of the two controllers.

Table 3. Case 1: Overshoot (OS), undershoot (US), and maximum settling time T_s for both controllers.

Controller	OS (rad/s)	US (rad/s)	Ts (ms)
Proposed Controller	3.12	2.8	21
PID	24	22.1	125

3.2. Case II—Robustness to sudden load torque changes with parameter uncertainties

To test the robustness of the two controllers to step load torque changes with the parameter uncertainties of Table 2, we assume that the converter is subjected to an external load torque change from 0.1 N.m to 0.2 N.m at t = 1 s and then back to 0.1 N.m at t = 2 s. The reference angular speed is ω_{ref} = 200 rad/s, and the input voltage is E = 50 V.

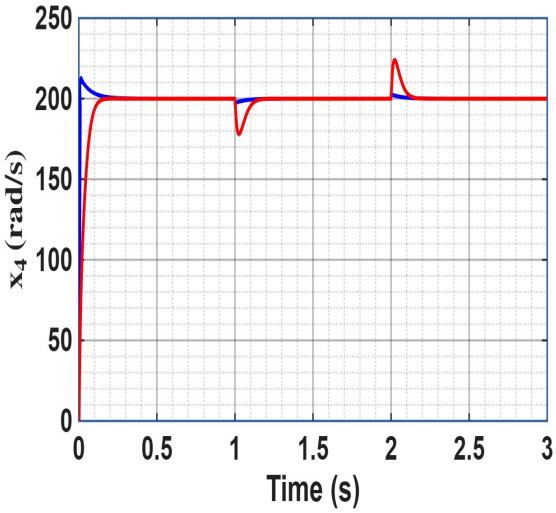

Figure 6. Case I: Angular speed response x_4 due to step input voltage changes with the proposed controller in blue and the PID in red.

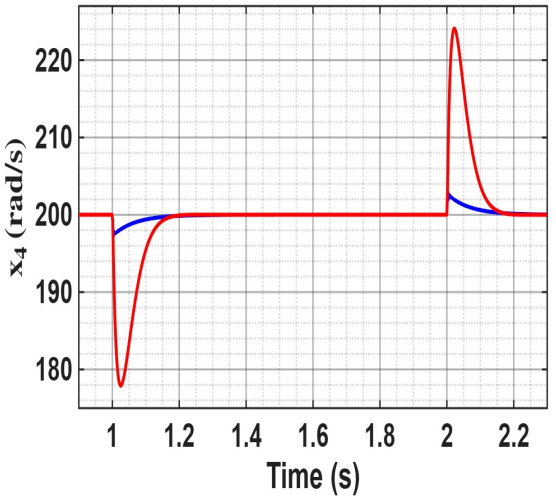

Figure 7. Case I: Zoom-in of Figure 6 of the angular speed response x_4 with the proposed controller in blue and the PID in red.

From the plots of the transient output responses depicted in Figures 8 and 9, the motor speed undergoes a maximum deviation of 6.10 rad/s (3.05%) with the disturbance completely rejected in less than 64 ms using the proposed controller. Using the PID controller, the motor speed undergoes a maximum deviation of 46.5 rad/s (23.25%) with the disturbance completely rejected in less than 134 ms. Table 4 summarizes the performances of the two controllers.

Table 4. Case II: Overshoot (OS), undershoot (US), and maximum settling time T_s for both controllers.

Controller	OS (rad/s)	US (rad/s)	T_s (ms)
Proposed Controller	6	6.1	64
PID	46.42	46.5	134

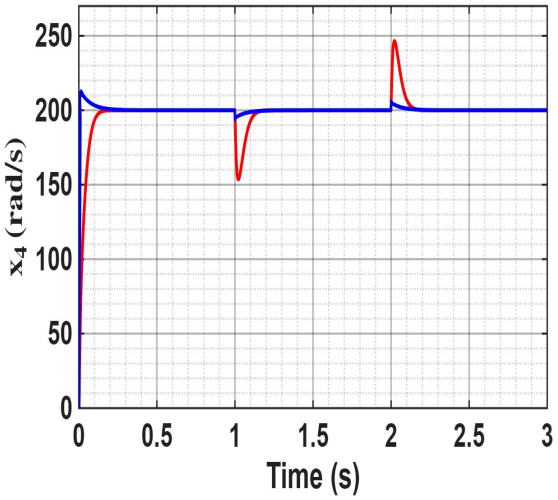

Figure 8. Case II: Angular speed response x_4 due to step load torque changes with the proposed controller in blue and the PID controller in red.

3.3. Case III—Robustness to time-varying input voltage, torque, and parameter uncertainties

To test the robustness of the two controllers to time-varying disturbances and parameter uncertainties, we assume that the converter/motor system is subjected simultaneously to the parameter uncertainties listed in Table 2, to a time-varying input voltage E, and a time-varying load torque τ shown in Figure 10. We assume a reference speed $\omega_{ref} = 200\ rad/s$. From the plots of the transient speed responses depicted in Figures 11 and 12, the motor speed undergoes a deviation of 5.16 rad/s (2.58%) with a DC offset error of 0.092 rad/s with the proposed controller. Using the PID controller, the motor speed undergoes a deviation of 29.8 rad/s (14.9%) with a DC-offset error of approximately 0.8 rad/s.

As seen in these simulations, both controllers exhibit excellent features in terms of achieving very stable and accurate speed control tracking under a parasitic of the converter and parameter uncertainties. During step input voltages and step input torques, the proposed controller outperforms the PID controller in achieving substantially lower speed deviations and recovery time. Furthermore,

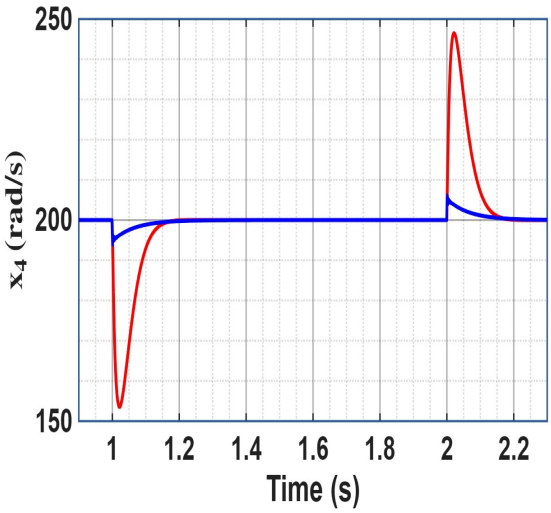

Figure 9. Case II: Zoom-in of Figure 8 of the angular speed response x_4 with the proposed controller in blue and the PID in red.

for time varying disturbances, the proposed controller yields a much smaller speed deviation and a smaller DC error between the reference speed and the actual speed than the PID controller.

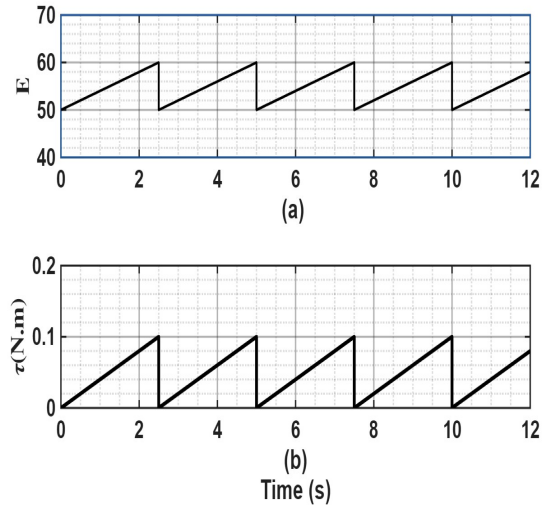

Figure 10. Case III: (a) Time-varying input voltage E and (b) time-varying load torque τ.

3.4. Case IV— Further robustness tests to large parameter uncertainties

In this test, we are simulating Case II with all the nominal parameters of the converter and the motor increased by 100% and then reduced by 80% from their nominal values listed in Table 1. For extreme parameter variations, the adaptation law gain γ should typically be chosen small to avoid oscillations in the speed response. In this case, we chose $\gamma = 5$, with K_4 and K_s unchanged.

As seen in Figures 13 and 14, the proposed controller achieves very accurate speed tracking despite the extreme variations of the converter and motor parameters from their nominal values. The

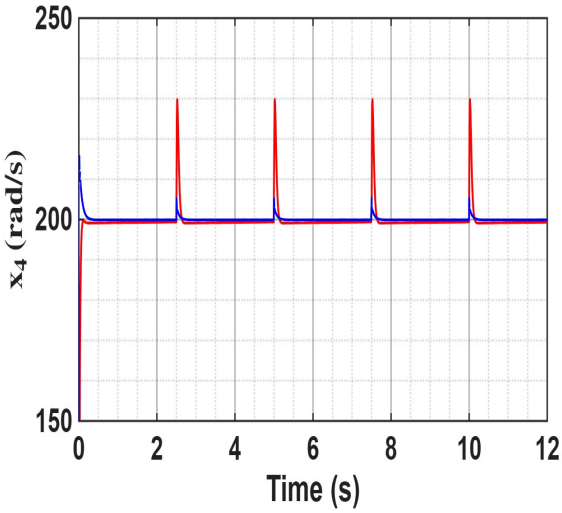

Figure 11. Case III: Angular speed response x_4 due to time-varying input voltage and load torque shown in Figure 10 with the proposed controller in blue and the PID controller in red.

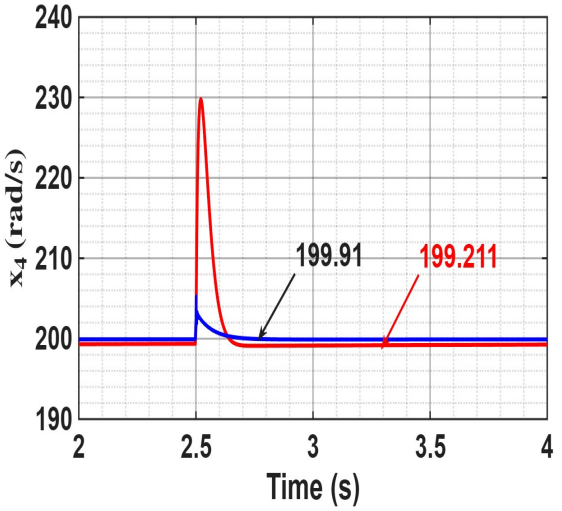

Figure 12. Case III: Zoom-in from Figure 11 of the angular speed response x_4 with the proposed controller in blue and the PID in red.

rigorous mathematical proof of the robustness of the proposed controller to maintain very accurate speed tracking under all possible variations of the ten parameters is a very difficult task for the four-dimensional system and, to the best of our knowledge, such rigorous analysis has not appeared in the literature and will be investigated in future work. Future work will also include running extensive Monte Carlo analysis and global sensitivity analysis using the Morris method. Remark 5 has been added to give an insightful explanation of how accurate speed tracking is achieved despite the presence of uncertainties.

Remark 5: The buck converter is subjected to the following parameter uncertainties:

$$\begin{gathered} L = L_o + \Delta L,\ C = C_o + \Delta C, \\ R = R_o + \Delta R, R_L = R_{Lo} + \Delta R_L \end{gathered} \tag{36}$$

and the parameter uncertainties of the DC motor are

$$\begin{gathered} R_a = R_{ao} + \Delta R_a,\ L_a = L_{ao} + \Delta L_a, \\ k_e = k_{eo} + \Delta k_e,\ k_m = k_{mo} + \Delta k_m, \\ D = D_o + \Delta D,\ J = J_o + \Delta J \end{gathered} \tag{37}$$

where the subscript "o" denotes the nominal value of the particular parameter under consideration. In this case, the same observer (3) is used with the known nominal values

$$\begin{gathered} \dot{\hat{x}}_1 = -\frac{R_{Lo}}{L_o}\hat{x}_1 - \frac{\hat{x}_2}{L_o} + u\frac{E}{L_o} \\ \dot{\hat{x}}_2 = \frac{\hat{x}_1}{C_o} - \frac{\hat{x}_2}{R_o C_o} - \frac{\hat{x}_3}{C_o} \\ \dot{\hat{x}}_3 = \frac{\hat{x}_2}{L_{ao}} - \frac{R_{ao}}{L_{ao}}\hat{x}_3 - \frac{k_{eo}}{L_{ao}}\hat{x}_4 \end{gathered} \tag{38}$$

$$\dot{\hat{x}}_4 = \frac{k_{mo}}{J_o}\hat{x}_3 - \frac{D_o}{J_o}\hat{x}_4 - \frac{\hat{\tau}}{J_o} + K_4(x_4 - \hat{x}_4)$$

with the adaptation law

$$\dot{\hat{\tau}} = -\gamma\frac{k_{eo}}{k_{mo}}\tilde{x}_4 \tag{39}$$

and the controller (13) with known nominal values is

$$u = \frac{\hat{x}_2 + R_{Lo}\hat{x}_1 + L_o\alpha_o\dot{\hat{\tau}}}{E} - \frac{K_s}{E}\sigma \tag{40}$$

where $\alpha_o = \dfrac{(1 + \frac{R_{ao}}{R_o})}{k_{mo}}$

with the estimated equilibrium

$$\begin{aligned}\hat{x}_1^* &= \frac{\hat{x}_2^*}{R_o} + \hat{x}_3^* \\ \hat{x}_2^* &= R_{ao}\hat{x}_3^* + k_{eo}x_4^* \\ \hat{x}_3^* &= \frac{D_o x_4^* + \hat{\tau}}{k_{mo}} \\ \hat{u}^* &= \frac{\hat{x}_2^* + R_{Lo}\hat{x}_1^*}{E}\end{aligned} \tag{41}$$

The application of the sliding surface (10), observer (38), adaptation law (39), and controller (40) on system (1) described with actual parameters still yields

$$\begin{aligned}\hat{x}_1 = \hat{x}_1^*,\ \hat{x}_2 \to \hat{x}_2^*, \\ \hat{x}_3 \to \hat{x}_3^*,\end{aligned} \tag{42}$$

with the $\hat{x}_1^*$, $\hat{x}_2^*$, and $\hat{x}_3^*$ given in (41).

The equilibrium point depends on the external load torque. In the case of known converter/motor parameters, it was proven that the estimation errors as well as the external load torque estimation error converge to zero and the estimated equilibrium converge to the true equilibrium as seen in Figures 17 and 18.

In the case of uncertain parameters, there is a steady-state error of the load torque estimate $\hat{\tau}$ from its true value τ as seen in Figure 15 and coupled with parameter uncertainties, the estimated equilibrium (41) does not converge to the true equilibrium given in (2). The estimation errors $\tilde{x}_1, \tilde{x}_2$, and $\tilde{x}_3$ are no longer zeros as seen in Figure 16. Also seen in Figure 16, is the satisfaction of (42). However, it is the presence of the steady-state error between $\hat{\tau}$ from its true value τ that will absorb the effect of the parameter uncertainties and accordingly change the estimates $\hat{x}_1 = \hat{x}_1^*$ and $\hat{x}_2 \to \hat{x}_2^*$ in controller (40) to maintain perfect tracking in the presence of uncertainties. Please see the duty ratio u for the nominal parameters in Figure 17 and the duty ratio u for a 100% parameter increase in Figure 15.

4. Conclusions

The salient features of this work are the simplicity of the design and the ease of implementation of the proposed adaptive controller that requires only one sensor. A detailed analysis of the closed-loop stability with nominal parameters and a simple procedure that systematically determines the three controller parameters are presented. Its robustness and effectiveness is validated by computer simulations and compared to the PID controller. Future work will involve the validation of the controller experimentally.

Author contributions

Said Oucheriah: Conceptualization, methodology, software, validation, formal analysis, writingoriginal draft preparation. Abul Azad: Validation, writing-review and editing, supervision, project administration, funding acquisition. All authors have read and approved the final version of the manuscript.

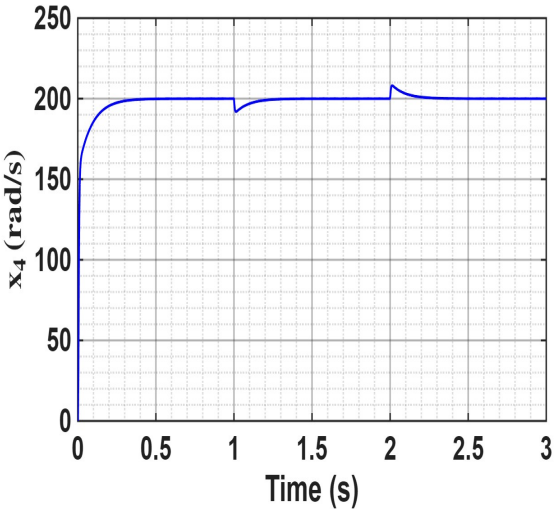

Figure 13. Case IV: Angular speed response x_4 with the parameters of the converter and motor increased by 100% from their nominal values listed in Table 1.

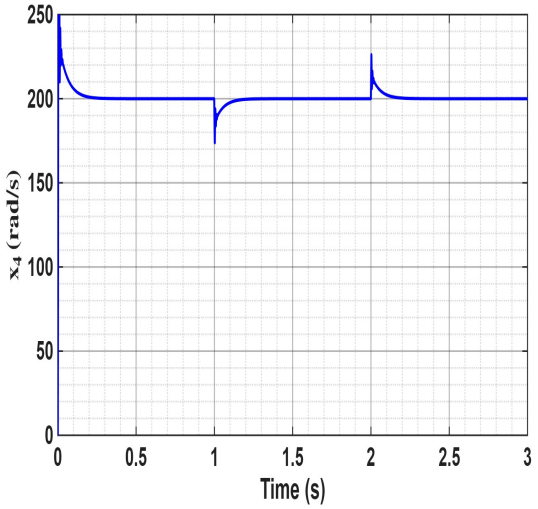

Figure 14. Case IV: Angular speed response x_4 with the parameters of the converter and motor decreased by 80% from their nominal values listed in Table I.

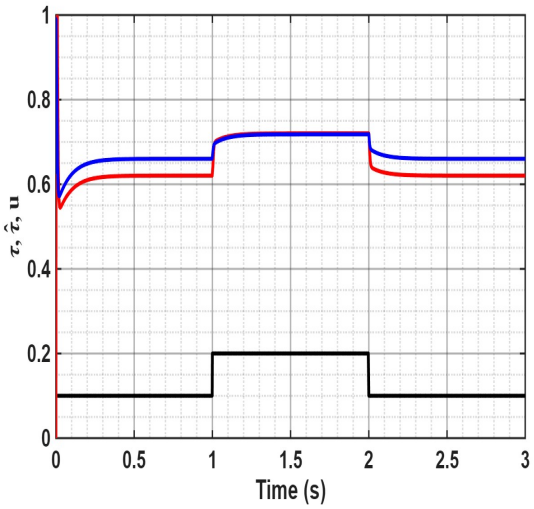

Figure 15. Case IV: External torque τ in black, estimated torque $\hat{\tau}$ in red, and the duty ratio u in blue with a 100% converter/motor parameter increase.

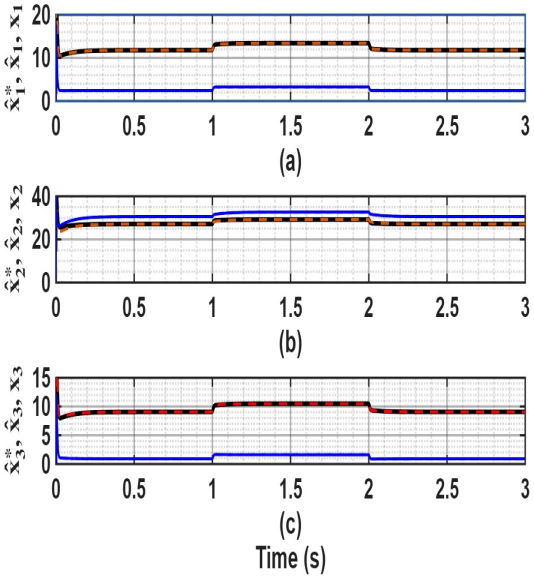

Figure 16. Case IV: Estimated states, estimated equilibrium, and actual states: (a) $\hat{x}_1^*$ in black, $\hat{x}_1$ in red, and x_1 in blue; (b) $\hat{x}_2^*$ in black, $\hat{x}_2$ in red, and x_2 in blue; (c) $\hat{x}_3^*$ in black, $\hat{x}_3$ in red, and x_3 in blue with a 100% converter/motor parameter increase.

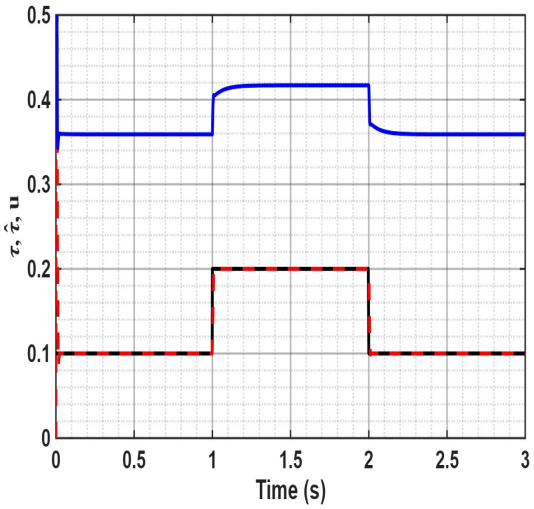

Figure 17. Case IV: External torque τ in black, estimated torque $\hat{\tau}$ in red, and the duty ratio u in blue with the known nominal converter/motor parameters of Table 1.

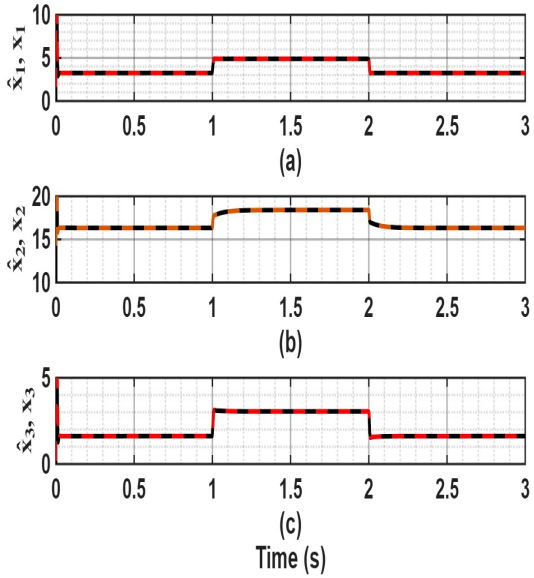

Figure 18. Case IV: Estimated states and actual states: (a) $\hat{x}_1$ in red and x_1 in black; (b) $\hat{x}_2$ in red and x_2 in black; (c) $\hat{x}_3$ in red, and x_3 in black with the known nominal motor/converter parameters of Table 1.

Use of Generative-AI tools declaration

The authors declare they have not used Artificial Intelligence (AI) tools in the creation of this article.

Conflict of interest

The authors declare that there is no competing financial interest that could have appeared to influence the work reported in this paper.

References

1. Hernandez-Marquez E, Silva-Ortigoza R, Garcia-Sanchez JR, Marcelino-Aranda M, Saldana-Gonzalez G (2018) A DC/DC Buck-Boost Converter-Inverter-DC Motor System: Sensorless Passivity-Based Control. *IEEE Access* 6: 31486–31492. https://doi.org/10.1109/ACCESS.2018.2846614
2. Yang J, Wu H, Hu L, Li S (2019) Robust Predictive Speed Regulation of Converter-Driven DC Motors via a Discrete-Time Reduced-Order GPIO. *IEEE Transactions on Industrial Electronics* 66: 7893–7903. https://doi.org/10.1109/TIE.2018.2878119
3. Agarwal J, Parmar G, Gupta R, Sikander A (2018) Analysis of grey wolf optimizer based fractional order PID controller in speed control of DC motor. *Microsystem Technologies* 24: 4997-5006. https://doi.org/10.1007/s00542-018-3920-4
4. Peicheng S, Suo W, Rongyun Z, Ping X (2019) Study on the fuzzy proportional-integral-derivative direct torque control strategy without flux linkage observation for brushless direct current motors. *International Journal of Advanced Robotic Systems* 16: 1729881419853141. https://doi.org/10.1177/1729881419853141
5. Hu H, Wang T, Zhao S, Wang C (2019) Speed control of brushless direct current motor using a genetic algorithm-optimized fuzzy proportional integral differential controller. *Advances in Mechanical Engineering* 11: 1687814019890199. https://doi.org/10.1177/1687814019890199
6. Hekimoglu B (2019) Optimal Tuning of Fractional Order PID Controller for DC Motor Speed Control via Chaotic Atom Search Optimization Algorithm. *IEEE Access* 7: 38100–38114. https://doi.org/10.1109/ACCESS.2019.2905961
7. Rigatos G, Siano P, Sayed-Mouchaweh M (2020) Adaptive neurofuzzy H-infinity control of DC-DC voltage converters. *Neural Computing and Applications* 32: 2507–2520. https://doi.org/10.1007/s00521-019-04394-4
8. Rauf A, Li S, Madonski R, Yang J (2020) Continuous dynamic sliding mode control of converter-fed DC motor system with high order mismatched disturbance compensation. *Transactions of the Institute of Measurement and Control* 42: 2812–2821. https://doi.org/10.1177/0142331220933415
9. Silva-Ortigoza R, Hernández-Márquez E, Roldán-Caballero A, Tavera-Mosqueda S, Marciano-Melchor M, Garcia-Sanchez JR, et al. (2021) Sensorless tracking control for a "full-bridge Buck inverter-DC motor" system: Passivity and flatness-based design. *IEEE Access* 9: 132191–132204. https://doi.org/10.1109/ACCESS.2021.3112575

10. Silva-Ortigoza R, Marciano-Melchor M, García-Chávez RE, Roldán-Caballero A, Hernández-Guzmán VM, Hernández-Márquez E, et al. (2022) Robust Flatness-Based Tracking Control for a "Full-Bridge Buck Inverter–DC Motor" System. *Mathematics* 10: 4110. https://doi.org/10.3390/math10214110
11. Kim PS, Kim SY (2022) A DC Motor Speed Control System with Disturbance Rejection and Noise Reduction. *IAENG International Journal of Applied Mathematics* 52: 918–927.
12. Ibrahim EK, Abbas AH, Gitaffa SA (2022) Optimization and Performance Analysis of Fractional Order PID Controller for DC Motor Speed Control. *Journal Européen des Systèmes Automatisés* 55: 723–739. https://doi.org/10.18280/jesa.550605
13. García-Chávez RE, Silva-Ortigoza R, Hernández-guzmáN VM, Marciano-Melchor M, Orta-Quintana ÁA, García-Sánchez JR, et al. (2023) A Robust Sliding Mode and PI-Based Tracking Control for the MIMO DC/DC Buck Converter-Inverter-DC Motor System. *IEEE Access* 11: 119396–119408. https://doi.org/10.1109/ACCESS.2023.3327425
14. Ravikumar D, Srinivasan GK (2023) Implementation of higher order sliding mode control of DC-DC buck converter fed permanent magnet DC motor with improved performance. *Automatika* 64: 162–177. https://doi.org/10.1080/00051144.2022.2119499
15. Roldán-Caballero A, Hernández-Marquez E, Marciano-Melchor M, García-Sánchez JR, Silva-Ortigoza G (2023) Hierarchical Flatness-Based Control for Velocity Trajectory Tracking of the DC/DC Boost Converter-DC Motor System Powered by Renewable Energy. *IEEE Access* 11: 32464–32475. https://doi.org/10.1109/ACCESS.2023.3260188
16. Ahmed A, Roy NK, Mahmud K (2024) Achieving Robust and Optimal Speed Control of DC Motor through Sliding Mode Control Tuned by Genetic and Particle Swarm Optimization Algorithms. *Smart Grids and Sustainable Energy* 9: 35. https://doi.org/10.1007/s40866-024-00223-3
17. Montoya-Acevedo D, Gil-Gonzalez W, Montoya OD, Restrepo C, Gonzalez-Castano C (2024) Adaptive Speed Control for a DC Motor Using DC/DC Converters: An Inverse Optimal Control Approach. *IEEE Access* 12: 154503–154513. https://doi.org/10.1109/ACCESS.2024.3482982
18. Almawla AA, Hussein MJ, Abdullah AT (2024) A Comparative Study of DC Motor Speed Control Techniques Using Fuzzy, SMC and PID. *Journal Européen des Systèmes Automatisés* 57: 397–406. https://doi.org/10.18280/jesa.570209
19. Sonugur G (2025) Efficient speed control of DC motors: imitation learning with fuzzy logic expert systems. *Automatika* 66: 306–320. https://doi.org/10.1080/00051144.2025.2480425
20. Acevedo DM, Parraguez-Garrido I, Gil-González W, Montoya OD, González-Castaño C (2025) Adaptive Passivity-Based Control for DC Motor Speed Regulation in DC-DC Converter-Fed Systems. *IEEE Access* 13: 131957–131966. https://doi.org/10.1109/ACCESS.2025.3592594
21. Pandya H, Vyas DR, Thakar PS, Markana A, Prajapati S (2025) Improved Robust and Optimal Performance of DC Servo Motor Using Model Predictive Control With Implementation. *Advanced Control for Applications: Engineering and Industrial Systems* 7: e70024. https://doi.org/10.1002/adc2.70024
22. Montoya-Acevedo D, Montoya OD, Garces-Ruiz A, Gonzalez-Castano C, Restrepo C (2025) Continuous Control-Set Model-Predictive Control for a Series-Wound DC Motor Drive. *IEEE Transactions on Industrial Electronics* 99: 1–11. https://doi.org/10.1109/TIE.2025.3637340

23. Maghfiroh H, Saputro JS, Ramelan A, Ma'arif A, Ibrahim IA, Latifa S (2026) Basic Tutorial on Model Predictive Control for Speed Control of DC-motor. *International Journal of Robotics and Control Systems* 6: 1–15. https://doi.org/10.31763/ijrcs.v6i1.1966

24. Elvira-Ceja S, Valderrabano-Gonzalez A, Castaneda CE, Gabbar HA (2026) Real-Time Speed Regulation of Direct Current Electric Motors Controlled by an Electric Motor Drive System Based on Diverse Power Converter Topologies. *Applied Sciences* 16: 1357. https://doi.org/10.3390/app16031357

AIMS Press